Electron heating effect on self-induced-transparency threshold in ultra-intense laser pulse interaction with overdense plasmas

E. Siminos[1], M. Grech[1], S. Skupin[1,2], T. Schlegel[3], and V. T. Tikhonchuk[4]

[1]*Max Planck Institute for the Physics of Complex Systems, D-01187 Dresden, Germany*

[2]*Friedrich Schiller University, D-07743 Jena, Germany*

[3]*Helmholtz Institute Jena, D-07743 Jena, Germany*

[4]*Centre Lasers Intenses et Applications, F-33405 Talence, France*

Abstract

Restricting attention to circularly-polarized pulses, we undertake a systematic comparison of 1D-3V PIC-simulation results to predictions of a cold-fluid model for the threshold of relativistic self induced transparency in overdense plasmas. We find that kinetic effects, such as longitudinal electron heating, dominate the process at high laser intensity, causing electrons to escape into the vacuum and leading to an increase of the effective critical density compared to the predictions of the cold-fluid model. We interpret our results through a dynamical systems' study of single electron phase space at the plasma-vacuum interface.

Introduction

For relativistically intense laser pulses (intensity $\mathrm{I} \gtrsim 10^{18}\,\mathrm{W\,cm^{-2}}$ for 1μm wavelength), the question of whether a pulse of frequency ω_L propagates in a plasma of density n_0, cannot be answered solely in terms of the critical density, $n_c = \varepsilon_0 m_e \omega_L^2/e^2$, where m_e is the electron mass, $-e$ is the electron charge, and ε_0 is the permittivity of free space. Taking relativistic effects into account, one usually introduces an effective critical density [1], $n_c^{\mathrm{eff}} = \sqrt{1+\frac{a_0^2}{2}}\,n_c$, where $a_0 = eA_0/m_e c$ is the normalized amplitude of the laser vector potential.

Thus, a relativisticly intense laser pulse can propagate in a nominally overdense plasma, a phenomenon known as *relativistic self-induced transparency* (RSIT). Apart from its role as a fundamental process in laser-plasma interaction, RSIT is also interesting for applications. In the context of ion acceleration, for instance, RSIT can prevent efficient ion radiation-pressure-acceleration. However, several factors, such as laser polarization [2] and boundary conditions at the plasma-vacuum interface [2, 3, 4], play a role in determining the effective critical density. In this work, the focus will be on kinetic effects.

For circularly polarized (CP) pulses, normal incidence, 1D3V geometry and immobile ions, relativistic cold-fluid theory predicts stationary solutions which correspond to either propagation, or total reflection with formation of a standing wave at the plasma boundary [2, 3, 4]. The

range of existence of standing wave solutions has been studied in Refs. [3, 4] and it defines the threshold density $n_{\rm th}(a_0)$ below which RSIT is possible for a given a_0, see Fig. 1.

Whether the initial density n_0 is larger or lower than $n_{\rm th}$, cold-fluid theory suggests [4] and PIC simulations confirm [4, 5] that for pulses with a finite rising time, at the initial stages of interaction, the ponderomotive force pushes the electrons deeper into the plasma, creating a charge separation layer (CSL) and a compressed electron layer (CEL) at the edge of the plasma, where the ponderomotive force is balanced by the electrostatic field due to charge separation. The density in the CEL is typically much higher than $n_c^{\rm eff}$ and the pulse cannot propagate. For $n_0 < n_{\rm th}$, where standing wave solutions are not predicted by the cold-fluid theory, PIC simulations [4, 5] show that electrons at the edge of the CEL escape towards the vacuum, resulting in force imbalance and penetration of the pulse deeper into the plasma.

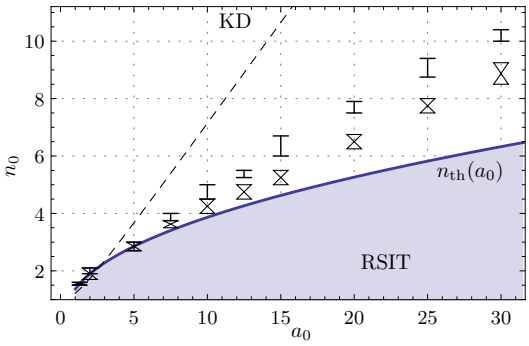

Figure 1: Effective critical density $n_{\rm th}$ as a function of laser field amplitude a_0 as predicted by cold-fluid theory [3, 4], (solid blue line), by Kaw and Dawson's relation $n_c^{\rm eff} = \sqrt{1+\frac{a_0^2}{2}}\,n_c$ (dashed black line) and as obtained from our PIC simulations, with two different pulse rising times: $0.25\tau_L$ (errorbars) and $4\tau_L$ (triangular errorbars), $\tau_L = 2\pi/\omega_L$. The shaded area represents the region within which RSIT is possible according to the cold-fluid model. In our normalization the laser intensity is $a_0^2/2$.

In the present study we show, through PIC simulations, that, in the presence of electron heating, such a propagating front mechanism can be activated by electrons escaping towards the vacuum, even for densities $n_0 > n_{\rm th}(a_0)$, see Fig. 1. However, in this regime, *infinitesimally* perturbing electrons at the edge of the plasma won't force them to leave the target [5], and one may still expect relaxation towards a stationary solution. To interpret our results, we are thus led to study the response of electrons at the edge of the CEL to *arbitrary* perturbations.

Electron phase space

The equations of motion for an electron in the region $x \le x_b$, in the case of full reflection, can be derived from the Hamiltonian $H(x,p_x) = \gamma(x,p_x) - \phi(x)$, where the electron γ factor reads $\gamma = \sqrt{1+a^2(x)+p_x^2}$, p_x is the electron's longitudinal momentum, and the electrostatic $\phi(x)$ and vector potential $a(x)$ are given by [3]

$$\phi(x) = \begin{cases} 0\,, & x < 0\,, \\ -\frac{1}{2}n_0 x^2, & 0 \le x \le x_b\,, \end{cases} \tag{1}$$

and

$$a(x) = \sqrt{2}a_0 \sin\left[\arcsin\left(\frac{a_b}{\sqrt{2}a_0}\right) - (x - x_b)\right], \tag{2}$$

respectively, with $a_b \equiv a(x_b)$, x_b being the boundary of the CEL.

The Hamiltonian $H(x, p_x)$ is a conserved quantity and we can thus write an explicit expression for the phase space characteristics for initial conditions x_0, p_{x0}:

$$p_x(x) = \pm\sqrt{[H(x_0, p_{x0}) + \phi(x)]^2 - a^2(x) - 1}\,. \tag{3}$$

Equation (3) suffices to plot portraits of the single-electron phase space, as in Fig. 2.

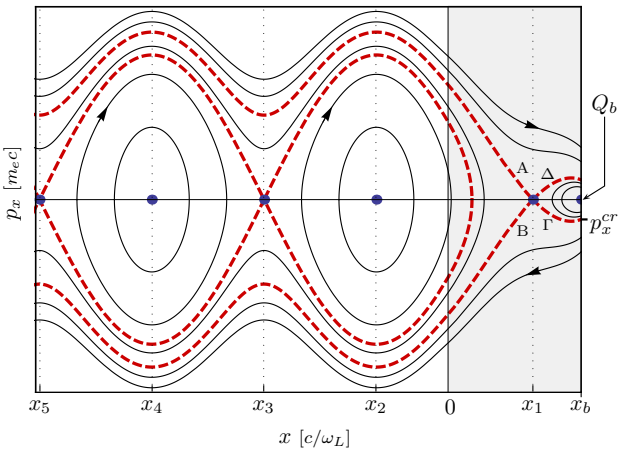

Figure 2: Typical single electron phase-space portrait for electrons in the CEL and vacuum. Equilibria are shown as blue dots, separatrices as red, dashed lines and some typical trajectories as black, solid lines.

Of greatest importance in the following are the separatrices labeled Γ and Δ, as they determine the region within which motion close to the equilibrium point $Q_b \equiv (x_b, 0)$ is oscillatory. The point on separatrix Γ at position x_b (at the plasma boundary) defines a momentum $p_x^{cr} \equiv p_x(x_b)$, which can be calculated from Eq. (3) with $(x_0, p_{x0}) = (x_1, 0)$. If a single electron at the edge of the CEL, x_b, is given an initial momentum $-|\Delta p_x|$, with $|\Delta p_x| < |p_x^{cr}|$, it will move within the limits set by separatrices Γ and Δ, returning back to the plasma. If on the other hand $|\Delta p_x| > |p_x^{cr}|$, the electron's motion will be unbounded and it will escape to the vacuum. It can be shown that $|p_x^{cr}| \to 0$ as $n_0 \to n_{th}$, for a fixed a_0.

It now becomes clear that finite perturbations of initial conditions of electrons at the edge of the plasma, for example due to heating, could lead to electrons escaping towards the vacuum, eventhough the equilibrium $Q_b \equiv (x_b, 0)$ is stable in the linear approximation.

Simulations

To investigate the threshold between total reflection and RSIT, we perform Particle-In-Cell (PIC) simulations using the one-dimensional in space, three-dimensional in velocity (1D3V) code SQUASH. The plasma extents from $x = 0$ to $x = L_p$, with a step-like density profile of constant density n_0 and temperature $T_0 \simeq 5 \cdot 10^{-4}$ (in units of $m_e c^2$). The circularly polarized laser pulse is incident from $x < 0$ onto the plasma. The laser pulse profile is trapezoidal, i.e. the intensity increases linearly within a rising time τ_r, up to a maximum value $a_0^2/2$.

For a typical case of full reflection, the phase space portraits of Fig. 3(a)-(d), show that the minimum momentum, $p_x^{\min}$, attained by electrons is smaller in absolute value than the momentum required to move beyond the limits set by the separatrices of bounded and unbounded motion, $|p_x^{\min}| < |p_x^{\rm cr}|$. Thus, electrons which cross the plasma boundary x_b do not escape into the vacuum but rather re-enter the plasma.

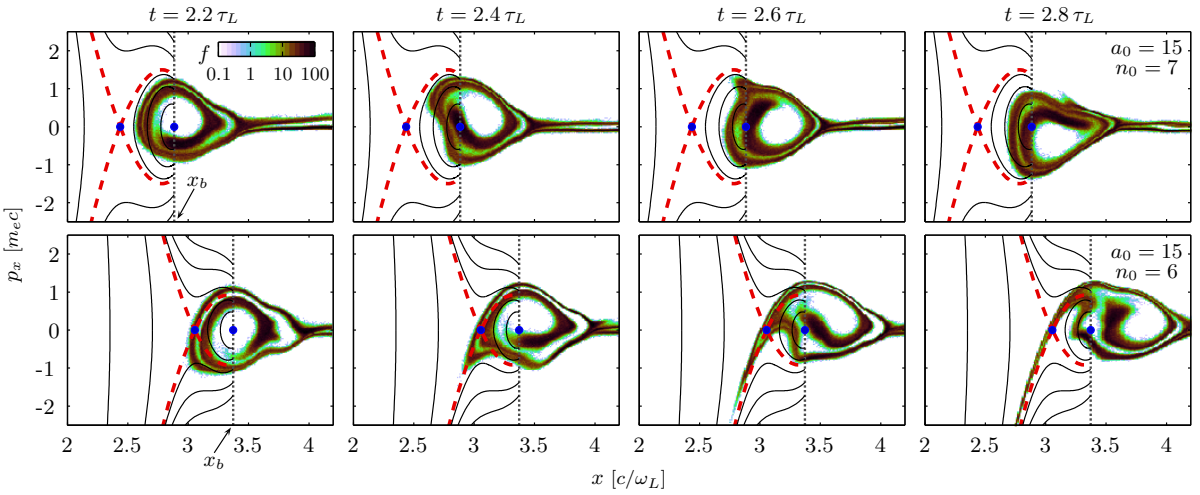

Figure 3: Comparison between phase space separatrices as predicted by the stationary, cold-fluid model, and $f(x,v)$ from PIC simulation results for $a_0 = 15$ and $n_0 = 7$ (top panel), $n_0 = 6.0$ (bottom panel) and rising time $\tau_r = 0.25\,\tau_L$. The plasma boundary ($x = x_b$), as predicted by the cold-fluid model, is indicated by a gray, dotted, vertical line.

A typical case in which RSIT occurs within the regime in which total reflection is predicted by the cold-fluid model, $n_0 > n_{\rm th}(a_0)$, is shown in Fig. 3(e)-(f). In this case, the minimum electron momentum satisfies $|p_x^{\min}| > |p_x^{\rm cr}|$ and electrons move outside the separatrix of bounded and unbounded motion, eventually reaching the vacuum.

Conclusions

We have used a dynamical systems' approach to bridge the cold-fluid and kinetic levels of RSIT description. Deviations of PIC simulations from cold-fluid theory predictions are explained as a longitudinal heating effect due to the pulse temporal profile.

References

[1] P. Kaw and J. Dawson. *Phys. Fluids* **13**, 472, 1970.

[2] J. H. Marburger and R. F. Tooper. *Phys. Rev. Lett.* **35**, 1001, 1975.

[3] F. Cattani, et al. *Phys. Rev. E* **62**, 1234, 2000.

[4] V. V. Goloviznin and T. J. Schep. *Phys. Plasmas* **7**, 1564, 2000.

[5] V. I. Eremin, et al. *Phys. Plasmas* **17**, 043102, 2010.